NASA Technical Paper 2281

February 1984

A Comparison of Two Position Estimate Algorithms That Use ILS Localizer and DME Information

Simulation and Flight Test Results

Charles E. Knox,
Dan D. Vicroy,
and Charles Scanlon

NASA

NASA
Technical
Paper
2281

1984

A Comparison of Two Position Estimate Algorithms That Use ILS Localizer and DME Information

Simulation and Flight Test Results

Charles E. Knox
and Dan D. Vicroy
Langley Research Center
Hampton, Virginia

Charles Scanlon
Arkansas State University
State University, Arkansas

NASA
National Aeronautics
and Space Administration

Scientific and Technical
Information Branch

SUMMARY

Flight tests with the Transport Systems Research Vehicle (TSRV) Boeing 737 airplane have shown that advanced forms of guidance presented on electronic flight displays may result in improved lateral and vertical tracking during the approach to landing. A critical element in producing the advanced guidance is the accuracy of the position estimate computed from inputs from radio navigation signals in the TSRV area navigation system. A comparison was made of the accuracy of two position estimation algorithms, each using a combination of instrument landing system (ILS) localizer and distance measuring equipment (DME) radio signals from an arbitrarily located DME facility to compute new estimates. One algorithm computes a position estimate with two independent error components, one from DME and the other from ILS localizer signals. The other algorithm computes a position estimate with a single error component, which is found by geometrically combining the output of both DME and ILS localizer signals.

Both simulation tests and flight tests using a radar tracker to determine flight path accuracy showed that an artificially induced position estimate error was reduced faster with the single-component solution than with the dual-component solution. Faster time constant gains were used in the position estimate filter for both algorithms to reduce position errors faster. A NASA test pilot reported that flight guidance based on the position estimate was smooth for all algorithm configurations and filter time constants tested.

A bias error was noted in the longitudinal axis (relative to the runway). This error was caused by a bias error within the DME indication. However, the bias error was well within the tolerances specified for the en route DME systems used during these tests. The resulting error may require the use of precision DME for guidance during the approach to landing segments of flight.

INTRODUCTION

Flight tests with the Transport Systems Research Vehicle (TSRV) Boeing 737 airplane flown in the microwave landing system (MLS) environment have shown that the TSRV area navigation system can provide situation and guidance information, in the form of a cathode ray tube (CRT) map display and a computer-drawn perspective runway symbol on the primary flight display (fig. 1), which results in improved pilot lateral and vertical tracking during the landing approach (refs. 1 and 2). A critical element in producing this advanced guidance was the accurate estimate of airplane position computed from the MLS signals by the navigation system. However, MLS is not yet commonly available at most airports; thus other forms of radio navigation aids will be required to determine airplane position if an earlier implementation of these advanced display concepts is desired.

The instrument landing system (ILS) is a precision radio navigation aid available at many airports. However, the ILS provides lateral information in the horizontal plane in the form of angular deviation relative to the runway centerline. This information must be combined with range information to completely define airplane horizontal position relative to the runway. An initial attempt was made to compute the position estimate with an algorithm that determined two independent

position difference components, one from ILS localizer signals and the other from DME signals. The ILS-based component was perpendicular to the runway centerline and the DME-based component was on a line between the airplane and the DME ground station. These components were used as inputs to the position estimate filter in the area navigation system. Although the design used in this first algorithm resulted in a more accurate position estimate than was normally obtained with the dual-DME position estimate mode (ref. 3), it did not provide sufficient accuracy for the pilots to use the advanced display symbology for primary guidance during an approach to landing.

To improve the accuracy of the position estimate, a second algorithm (originally documented in ref. 4) was designed for the TSRV 737 airplane navigation system. This algorithm used both ILS and DME information to compute a single position difference component for the position estimate filter. The locations of the ILS localizer and DME antennas were stored in the navigation data base and azimuthal information from the ILS localizer was geometrically combined with distance information from an arbitrarily located DME station to calculate position. The output of this geometric calculation was used as an input to the position estimate filter to produce a smoothed estimate on which display guidance could be based.

Simulation tests were conducted to adjust the filter time constants so that large position estimate errors occurring during en route flight would be nulled quickly while maintaining a smooth display of guidance to the pilot during transition into the ILS environment. Flight tests were conducted with the TSRV 737 airplane in a ground-based radar tracking environment to document the difference between the actual position of the airplane (radar defined) and the area navigation system position estimate. The purposes of this report are to document the equations and logic used to generate the position estimate with the ILS and DME information and to discuss the results of these simulation and flight tests.

SYMBOLS

A	distance between the DME and ILS localizer antenna, n.mi.
a	east component of A, n.mi.
b	north component of A, n.mi.
D_t	distance from DME to airplane corrected for slant range, n.mi.
D'_t	slant range distance from DME to airplane, n.mi.
$\overrightarrow{DP}$	position difference vector
$\overrightarrow{DP}_p$	component of position difference vector $\overrightarrow{DP}$ perpendicular to the runway centerline
DP_p	magnitude of vector $\overrightarrow{DP}_p$, n.mi.
F	ellipticity constant, 0.003367
h_a	altitude of airplane above mean sea level, ft
h_{DME}	altitude of DME antenna above mean sea level, ft

h_o altitude of ILS localizer antenna above mean sea level, ft

$\hat{i},\hat{j}$ unit coordinate vectors

K_1 position estimate filter gain

K_2 velocity estimate filter gain, hr^{-1}

K_3 velocity estimate filter gain

L outer radial limit of ILS localizer geometric check, n.mi.

M inner radial limit of ILS localizer geometric check, n.mi.

N,E axes of orthogonal coordinate system oriented toward true north

P angle formed by the vector $\vec{Z}_m$ and a line between the airplane and DME antenna, deg

r_E radius of Earth, ft

r_M meridional radius of curvature, n.mi.

r_N normal radius of curvature, n.mi.

$\hat{u}$ unit vector perpendicular to runway centerline

V_N,V_E north, east components of navigation system velocity estimate, knots

$\hat{V}_N,\hat{V}_E$ north, east components of inertial ground speed, knots

X',Y' axes of orthogonal coordinate system oriented along the runway centerline

X'_e,Y'_e coordinates of vector $\vec{Z}_e$ transformed into the X',Y' coordinate system

$\vec{Z}_e$ vector of estimated airplane position from ILS localizer antenna

Z_e magnitude of $\vec{Z}_e$, n.mi.

$Z_{e,N},Z_{e,E}$ north, east components of $\vec{Z}_e$, n.mi.

$\vec{Z}_m$ vector of measured position of airplane from the ILS localizer antenna

Z_m magnitude of $\vec{Z}_m$, n.mi.

$Z_{m,N},Z_{m,E}$ north, east components of position vector $\vec{Z}_m$, n.mi.

$\vec{Z}_r$ vector of estimated airplane position measured radially along ILS deviation angle

Z_r magnitude of position vector $\vec{Z}_r$, n.mi.

$Z_{r,N},Z_{r,E}$ north, east components of position vector $\vec{Z}_r$, n.mi.

α_t angle formed at ILS localizer antenna by DME antenna and measured airplane position, deg

β angle P limit at which DME inputs will be inhibited, deg

$\Delta P_N, \Delta P_E$ north, east components of position estimate difference, n.mi.

Δt computer iteration cycle, sec

$\Delta V_N, \Delta V_E$ north, east components of system velocity update, knots

$\Delta\phi, \Delta\lambda$ latitude, longitude update terms, deg

η localizer deviation angle relative to the runway centerline, deg

μ relative angle between the DME and the ILS localizer antenna, deg

$\phi_{DME}, \lambda_{DME}$ latitude, longitude of DME antenna location, deg

ϕ_e, λ_e latitude, longitude of estimated airplane position, deg

ϕ_o, λ_o latitude, longitude of ILS localizer antenna, deg

ϕ_r angle of runway centerline (opposite to direction of landing) relative to true north, deg

Ω vertical angular limit of ILS localizer geometric check, deg

ω lateral angular limit of ILS localizer geometric check, deg

Subscripts:

t at time t

t-1 at iteration time previous to time t

Abbreviations:

ACY Atlantic City DME navigation radio facility

CRT cathode ray tube

DME distance measuring equipment

IDD navigation position estimate mode: inertial velocity and dual DME

ILD navigation position estimate mode: inertial velocity, ILS localizer, and DME

ILS instrument landing system

ILX navigation position estimate mode: inertial velocity and ILS localizer

INS inertial navigation system

MSL	microwave landing system
NCU	navigation computer unit
rms	root mean square
TSRV	Transport Systems Research Vehicle
VCN	Cedar Lake DME navigation facility
VOR	very-high-frequency omnidirectional-range navigation radio

DESCRIPTION OF NAVIGATION POSITION ESTIMATE

General Description

The TSRV navigation computer was programmed to compute an estimate of airplane position and velocity based on combining data from an inertial navigation system (INS) and various radio navigation systems. Information from the airborne central air data computer and the magnetic direction system is also available in the event that INS information is unavailable.

Signals from the radio navigation systems are combined to determine airplane position. However, because of signal noise and various errors inherent within the radio navigation systems, this definition of airplane position must be combined with inertial velocity information from the INS in a position estimate filter to produce a smoothed estimation of airplane position. This estimate of position is computed at 20 Hz and is used as a basis for navigation, guidance, and display computations.

Various position estimate modes may be used, depending upon availability of the radio navigation signals. Position estimates normally are calculated with inputs from two different DME facilities for flights away from the terminal area. This position estimate mode is identified by the letters IDD (inertial velocity, DME, DME) shown on the electronic map display in front of each pilot. While the aircraft is operating in the terminal area and within signal coverage of an instrument landing system (ILS), the position estimate will be computed either with both ILS localizer and DME radio signals (ILD) or, if DME is not available, with localizer signals only (ILX).

In the TSRV navigation system, the radio signals are used to compute a position difference term to be used in the position estimate process. The position difference term is defined as the vector between the last previously estimated position and the position defined by the radio navigation information. The position difference vector is divided into north and east components, which are used as inputs in the position estimate filter. The equations used in the position estimate filter are given in appendix A.

ILS-DME (ILD) Position Estimate: Dual Component

The design of the first ILS position estimate algorithm involved simply substituting an ILS localizer input for one of the DME inputs in the conventional dual-DME position estimate algorithm. This resulted in two independent position difference components. The equations for the difference component computed with localizer

information are also used in the ILX mode and are described in appendix B. The equations for the difference component computed with the DME signal are described in reference 3. Each of these difference terms is resolved into north and east components, summed, and then used as input in the position estimate process.

ILS-DME (ILD) Position Estimate: Single Component

General solution.- Figure 2 shows the geometry of the ILS localizer antenna, the DME antenna, the airplane estimated position, the airplane position measured with localizer and DME information, and the runway with an extended centerline. An orthogonal coordinate system, with its origin placed on the localizer antenna, is oriented with respect to true north. Since the DME could be selected either manually or automatically, the position difference equations were derived so that the DME was not required to be collocated with the ILS localizer antenna.

By determining the relative geometry between the ILS localizer antenna, the DME antenna, and the position of the airplane measured with both localizer and DME information, the vector $\vec{Z}_{m,t}$ between the origin and the measured position of the airplane was found. The vector $\vec{Z}_{e,t-1}$ was found directly from the known latitudes and longitudes of the origin and the previously estimated position of the airplane. The position difference was then found by subtracting $\vec{Z}_{m,t}$ from $\vec{Z}_{e,t-1}$ and dividing into the north and east components $\Delta P_{N,t}$ and $\Delta P_{E,t}$.

Calculation of airplane position vector $\vec{Z}_{m,t}$.- Figure 2 shows that $\vec{Z}_{m,t}$ is one side of the triangle formed by the origin (ILS localizer antenna), the measured position of the airplane, and the DME antenna. Known quantities used to determine $\vec{Z}_{m,t}$ in this triangle include the angle of the runway centerline ϕ_r (opposite to the direction of landing), the slant range D_t' measured from the DME signals, the localizer deviation angle η_t relative to the runway centerline and measured from the ILS localizer signals, the location (latitude and longitude) ϕ_{DME},λ_{DME} of the DME antenna, and the location ϕ_o,λ_o of the ILS localizer antenna.

Figure 3 shows the angular geometry and distance A between the origin and the DME antenna. The length A and the angle μ between the DME antenna and the north axis remained constant for a particular DME and were calculated only once. If a different DME station was tuned, the A and μ were recalculated. The length of A was determined by vectorially summing its components a and b:

$$a = 60(\lambda_{DME} - \lambda_o) \cos \frac{\phi_o + \phi_{DME}}{2} \quad \text{n.mi.}$$

$$b = 60(\phi_{DME} - \phi_o) \quad \text{n.mi.}$$

$$A = \sqrt{a^2 + b^2} \quad \text{n.mi.}$$

The angle μ was found by

$$\mu = \tan^{-1}\left(\frac{a}{b}\right) \qquad (0 \leq \mu \leq 2\pi)$$

The angle α_t formed by side A and vector $\vec{Z}_{m,t}$ may vary continuously and was calculated 20 times per second. It ranged between 0 and π, inclusive, and was found by

$$\alpha_t = \left|2\pi - \mu + (\phi_r - \eta_t)\right|$$

If this calculated value of α_t was greater than π, then

$$\alpha_t = \left|2\pi - \left[\left|2\pi - \mu + (\phi_r - \eta_t)\right|\right]\right|$$

The value of the DME reading D'_t measured in the airplane was the slant range distance between the ground-based DME antenna and the airplane. This distance was corrected to determine the ground distance D_t shown in figure 3 between the airplane and DME:

$$D_t = D'_t \sin\left[\cos^{-1}\left(\frac{h_{a,t} - h_{DME}}{D'_t}\right)\right] \quad \text{n.mi.}$$

Angle P_t formed by the vector $\vec{Z}_{m,t}$ and side D_t could vary continuously and was calculated 20 times per second. From the relation

$$\frac{A}{\sin P_t} = \frac{D_t}{\sin \alpha_t} \quad \text{n.mi.}$$

angle P_t was determined by

$$P_t = \sin^{-1}\left(\frac{A}{D_t} \sin \alpha_t\right)$$

A comparison of the square of side A with the sum of the square of side D_t and the square of the magnitude of the vector $\vec{Z}_{e,t-1}$ was used to determine whether

angle P_t was obtuse or acute. (The airplane position vector estimated on the last iteration ($\vec{Z}_{e,t-1}$) was used as an approximation for $Z_{m,t}$.) Hence,

$$P_t = \begin{cases} \sin^{-1}\left(\frac{A}{D_t} \sin \alpha_t\right) & \left(A^2 \leq D_t^2 + Z_{e,t-1}^2\right) \\ \pi - \sin^{-1}\left(\frac{A}{D_t} \sin \alpha_t\right) & \left(A^2 > D_t^2 + Z_{e,t-1}^2\right) \end{cases}$$

The magnitude of the estimated airplane position vector $\vec{Z}_{e,t-1}$ was

$$Z_{e,t-1} = \left[(Z_{e,N,t-1})^2 + (Z_{e,E,t-1})^2\right]^{1/2} \quad \text{n.mi.}$$

in which

$$Z_{e,N,t-1} = 60(\phi_{e,t-1} - \phi_o) \quad \text{n.mi.}$$

$$Z_{e,E,t-1} = 60(\lambda_{e,t-1} - \lambda_o) \cos \frac{\phi_o + \phi_{e,t-1}}{2} \quad \text{n.mi.}$$

The magnitude of $\vec{Z}_{m,t}$ was then found as follows:

$$Z_{m,t} = A \cos \alpha_t + D_t \cos P_t \quad \text{n.mi.}$$

The north and east components of $\vec{Z}_{m,t}$ were calculated from the angle $\psi_r - \eta_t$ between the north axis and $\vec{Z}_{m,t}$:

$$Z_{m,N,t} = Z_{m,t} \cos(\psi_r - \eta_t) \quad \text{n.mi.}$$

$$Z_{m,E,t} = Z_{m,t} \sin(\psi_r - \eta_t) \quad \text{n.mi.}$$

Calculation of position difference in north and east components $\Delta P_{N,t}, \Delta P_{E,t}$.-

The position difference in north and east components was then found by subtracting

the north component of $\vec{Z}_{e,t-1}$ from the north component of $\vec{Z}_{m,t}$ and subtracting the east component of $\vec{Z}_{e,t-1}$ from the east component of $\vec{Z}_{m,t}$:

$$\Delta P_{N,t} = Z_{m,N,t} - Z_{e,N,t-1} \quad \text{n.mi.}$$

$$\Delta P_{E,t} = Z_{m,E,t} - Z_{e,E,t-1} \quad \text{n.mi}$$

These position difference components were then used directly in the navigation position estimate algorithms previously described.

ILS Localizer-Airplane Position Validity Check

Since random DME selection, automatic frequency tuning, and other means of automatic software control were utilized in the navigation computer, a check had to be made to ensure that the navigation computer was using the appropriate navigation data for the area in which the airplane was flying. Obviously, if improper navigation data were being utilized, position estimates based on those data would be inaccurate and should not be used.

To preclude the use of the wrong ILS localizer navigation data, a geometric check was made to determine whether the estimated position of the airplane was within the localizer boundaries. If the airplane was not within these boundaries, then ILS updating was inhibited. These boundaries included lateral and radial limits of coverage, as shown in figure 4. The lateral limit of the localizer angle of coverage is $\pm\omega$ from the runway centerline. Radial limits required that the airplane be within distance L of the localizer antenna, but not closer than distance M. A vertical angle of coverage limit Ω was measured from the localizer antenna.

A new orthogonal coordinate system, with its origin located at the ILS localizer antenna and its X'-axis on the runway centerline, was used to make the geometric check. The north and east components of the estimated position vector $\vec{Z}_{e,t-1}$ were transformed into the new X',Y' coordinate system as follows:

$$X'_{e,t} = Z_{e,N,t-1} \cos \psi_r + Z_{e,E,t-1} \sin \psi_r \quad \text{n.mi.}$$

$$Y'_{e,t} = Z_{e,N,t-1} \sin \psi_r - Z_{e,E,t-1} \cos \psi_r \quad \text{n.mi.}$$

The lateral azimuth check was then

$$-X'_{e,t} \tan \omega \leq Y'_{e,t} \leq X'_{e,t} \tan \omega \quad \text{n.mi.}$$

The radial check was

$$M \leq \frac{X'_{e,t}}{\cos \eta_t} \leq L \quad \text{n.mi.}$$

and the vertical check was

$$h_{a,t} \leq h_o + X'_{e,t} \tan \Omega$$

For these tests, the ILS localizer azimuth coverage limits were

Lateral, ω, deg	20
Vertical, Ω, deg	10
Inner radial, M, n.mi.	0.165
Outer radial, L, n.mi.	10

A geometric check of the location of the DME ground station relative to the airplane and the runway centerline is performed continuously to prevent the possibility of large position estimate errors caused by the DME inputs (fig. 5). As the angle P_t formed by the localizer antenna, airplane, and DME ground station approaches 90°, small errors from the DME range information can result in significantly larger radial position errors along the localizer deviation angle on which the airplane is located. Hence, if angle P_t falls within a prescribed angular boundary β about $P_t = 90°$, the DME signals will not be used and a new DME will be tuned or ILX updating will occur. This geometric check is defined as follows. If

$$\left(\frac{\pi}{2} + \beta\right) > P_t > \left(\frac{\pi}{2} - \beta\right)$$

then do not use DME information. For the simulation and flight tests documented in this report, $\beta = \pi/4$ or 45°.

DESCRIPTION OF SIMULATION, AIRBORNE FLIGHT SYSTEMS, AND GROUND-BASED RADAR

TSRV 737 Simulation

The TSRV 737 simulation consists of a fixed-base cockpit identical to the research flight deck in the TSRV airplane and a sophisticated, six-degree-of-freedom digital representation of the airplane and its experimental systems. Nonlinear effects such as engine response, varying stability functions, and control servo models, as well as modeling of the navigation, guidance, and display subsystems, are used to represent the research airplane with a high degree of realism.

Airborne Flight Systems

Airplane.- The NASA test airplane is the Boeing 737-100 twin-jet transport airplane shown in figure 6. The TSRV airplane is used as a research vehicle and has a complete set of experimental navigation, guidance, flight control, and display systems in a separate research cockpit located in the cabin of the airplane. All the normal flight systems (e.g., flight control, navigation, pressurization) have been retained in the conventional cockpit in a normal, functional state. This arrangement allows changes to be made to any of the experimental systems while retaining the standard operational features of the airplane.

Experimental systems.- The experimental research flight systems consist of a triplex digital flight control computer system, an electronic CRT display system, and a digital navigation and guidance system integrated into a separate, two-man-crew, research cockpit (ref. 3). The navigation and guidance calculations are performed in a single digital navigation computer. Various navigation sensor signals (including inertial navigation system velocities and accelerations, true airspeed, magnetic heading, and VOR, ILS, and DME radio signals) are used in the navigation computer. This computer estimates the airplane position based on combinations of the sensor inputs. Horizontal path, vertical path, and thrust guidance and commands based on the estimated position, estimated velocity, and path tracking errors of the airplane are displayed to the pilot on the CRT display system.

Airborne data acquisition system.- A wideband magnetic-tape recorder onboard the airplane recorded data at a rate of 40 samples per second. These data included 93 parameters describing the airplane configuration, attitude, and control surface activity. Thirty-two additional channels were used for recording navigation computer parameters, including the latitude and longitude of the navigation position estimate. Video recordings of the electronic attitude director and electronic horizontal-situation displays were also made throughout the flights.

Radar Tracking Facilities

Radar tracking of the airplane was provided by the Federal Aviation Administration Extended Area Instrumentation Radar (EAIR) Facility at the Federal Aviation Administration Technical Center (FAATC) in Atlantic City, New Jersey. The tracking radar is a precision C-band instrumentation radar system that was operated in a beacon-tracking mode during these flight tests. Slant range, azimuth angle, and elevation angle data were recorded on magnetic tape at a sample rate of 10 Hz. All airborne and ground-based recorded data were time correlated for postflight processing and analysis. Postflight processing of the range, azimuth, and elevation data consisted of conversion to latitude, longitude, and altitude.

Radar accuracy is stated (ref. 5) as 0.2 mrad, (0.011°) in azimuth and elevation angle and less than 20 yards rms error in range.

RESULTS AND DISCUSSIONS

Simulation Tests

Test procedure.- The TSRV 737 airplane simulation was used both in a fast-time mode without the research cockpit and in a real-time mode with a pilot operating the research cockpit. The fast-time mode was used to investigate the change in the

position estimate convergence characteristics for the single- and dual-component position difference solutions and to select gains for the position estimate filter. The real-time piloted mode was used to determine the effects that airplane maneuvers might have on the guidance based on the navigation position estimate.

Figure 7 is a plan view of the reference coordinate system, the runway, the DME antenna, and the localizer antenna modeled for the simulation. The origin of the reference coordinate system was located at the approach end of the runway with the x-axis oriented along the centerline of a north-south runway. The ILS localizer antenna and the DME antenna were collocated on the x-axis 8500 ft past the runway threshold (reference axis origin). This geometrical arrangement of the reference axes, runway alignment, and antenna locations was selected for these tests to facilitate data analysis. With this geometrical arrangement, the lateral component (east-west) of the position estimate was derived from ILS localizer signals and the longitudinal component (north-south) was derived from DME signals.

Fast-time simulation.- During the fast-time simulation tests, the airplane was constrained to fly along the ILS localizer toward the runway regardless of the navigation position estimate. At the start of each test, the navigation position estimate was offset to create a position estimate error of 1000 ft to the right and 1000 ft to the rear of the actual position of the airplane. The subsequent reduction of these errors was used to document the convergence characteristics for each test run. The position estimate error was broken into lateral and longitudinal components relative to the localizer centerline so that convergence due to ILS localizer information (lateral) and DME information (longitudinal) could be analyzed separately. The convergence characteristics for each component were quantified by the initial convergence rate, the time required to reduce the initial displacement error by 63 percent, and the resulting amount of overshoot.

The first four fast-time simulation runs were conducted to compare the convergence characteristics of the single-component solution with those of the dual-component solution. Each of these solutions was run with position estimate filter gains based on the 50 sec time constant normally used with dual-DME estimates (test condition 1) and with a faster, 30-sec time constant (test condition 2). The resulting lateral and longitudinal convergence characteristics for these runs and test conditions are tabulated in table I.

TABLE I.- LATERAL AND LONGITUDINAL CONVERGENCE CHARACTERISTICS OF ILS-DME POSITION ESTIMATE

[TSRV simulation; $K_3 = 1$]

Test condition	Component relative to localizer	Filter time constant, sec	Initial recovery rate, fps		63-percent recovery time, sec		Offset at threshold,* ft		Radio signal noise
			Dual component	Single component	Dual component	Single component	Dual component	Single component	
1	Lateral	50	20.5	38.0	45.0	23.7	-61.7	-46.9	No
2	Lateral	30	33.9	64.3	27.0	14.2	-80.8	-35.7	No
1	Longitudinal	50	40.1	39.1	22.8	23.6	-49.3	-52.0	No
2	Longitudinal	30	65.9	64.4	13.7	14.1	-45.6	-42.9	No

*Negative offset indicates an overshoot.

Table I shows that little change occurred in the longitudinal convergence characteristics between the single- and dual-component position difference solutions. This was expected because of the collocation of the DME and localizer antennas. In this geometric configuration, the magnitude of the position difference term was the same for each solution. Hence, the convergence characteristics were the same. Use of the 30-sec gains resulted in approximately 66 percent faster convergence than was obtained with the 50-sec gains.

The lateral convergence characteristics shown in table I indicate that use of the single-component position difference solution resulted in a faster reduction of error than was obtained with the dual-component solution. These results are illustrated in figure 8, which shows a time history trace of the initial 1000-ft lateral error and the subsequent recovery for each of the four runs. Use of the single-component solution resulted in an 85-percent increase in the initial lateral recovery rate (90 percent with the 30-sec time constant) and a 48-percent decrease in time to reduce the lateral error by 63 percent of the initial offset (47 percent with the 30-sec time constant). Overshoot occurred on all four runs. The overshoot was reduced from 80.8 ft with the dual-component solution to 35.7 ft with the single-component solution (30-sec time constant). However, it was felt that the overshoot occurring on all runs could result in flight crew confusion due to disagreement between guidance based on the navigation position estimate and guidance based on localizer deviation information.

The computations used to calculate the navigation system velocity estimate were examined to determine their effects on the position estimate convergence. The system velocity estimate is calculated by summing ground speed from the inertial navigation system with a comparatively small velocity correction term ($\Delta V_{N,t}$ and $\Delta V_{E,t}$) computed from the position difference defined by navigation radio information. This correction term is computed by summing a portion of the current position difference to the value that was computed on the last computation cycle ($K_3 = 1.0$) as follows:

$$\Delta V_{N,t} = K_3 \Delta V_{N,t-1} + K_2 \Delta P_{N,t} \quad \text{knots}$$

$$\Delta V_{E,t} = K_3 \Delta V_{E,t-1} + K_2 \Delta P_{E,t} \quad \text{knots}$$

Bias errors from the INS velocity inputs may be nulled over a period of time by accumulating a portion of the position error caused by the velocity error. However, when a large position step error is suddenly induced, as might be obtained when changing from en route navigation radio facilities to approach facilities, the velocity correction term will become great and could cause the navigation position estimate to momentarily undershoot or overshoot during the subsequent position error nulling process. The large position step error would eventually be nulled, but this would require more time than necessary to complete the approach to landing. In an effort to reduce the transient effects of large step errors the position estimate, the accumulation feature of the velocity estimate equation was removed by setting $K_3 = 0$.

The four fast-time simulation runs (test conditions 1 and 2) were repeated using the system velocity estimate equations with K_3 set equal to zero. The convergence characteristics resulting from these runs are quantified in table II. Figure 9 shows

TABLE II.- LATERAL AND LONGITUDINAL CONVERGENCE CHARACTERISTICS OF ILS-DME POSITION ESTIMATE USING MODIFIED SYSTEM VELOCITY ESTIMATE EQUATIONS

[TSRV simulation; $K_3 = 0$]

Test condition	Component relative to localizer	Filter time constant, sec	Initial recovery rate, fps		63-percent recovery time, sec		Offset at threshold,* ft		Radio signal noise
			Dual component	Single component	Dual component	Single component	Dual component	Single component	
1	Lateral	30	33.8	64.1	29.2	14.8	3.2	0.01	No
2	Lateral	50	20.4	39.0	48.7	24.7	33.5	1.0	No
3	Lateral	30	32.9	62.3	31.1	16.2	13.7	8.5	Yes
4	Lateral	50	19.9	37.9	51.4	26.5	44.5	10.7	Yes
1	Longitudinal	30	65.8	64.3	14.3	14.7	8.7	7.0	No
2	Longitudinal	50	40.0	39.1	23.8	24.6	8.5	6.9	No
3	Longitudinal	30	65.9	64.5	14.2	14.6	4.4	2.7	Yes
4	Longitudinal	50	40.2	39.2	23.6	24.4	2.5	0.3	Yes

*Positive offset indicates an undershoot.

the time history trace of the lateral component for each of these runs. These data indicate that the overshoot was substantially reduced. However, undershoot resulted in the run using the dual-component solution and the 50-sec filter gain. More time was required for nulling the lateral error with this solution and gain. The initial recovery rates were about the same as those obtained with the unmodified velocity estimate equations. The times required to reduce the initial displacement error by 63 percent were increased slightly due to the better estimate of system velocity computed with the modified equations.

Randomly generated noise was added to the simulated ILS localizer and DME radio signals to note any adverse effects on the convergence characteristics, particularly those obtained with the faster time constants. The four fast-time simulation runs were then repeated using the modified system velocity estimate equations (test conditions 3 and 4). The convergence characteristics resulting from these runs did not differ significantly from those without noise. The results are quantified in table II.

Real-time simulation.- A NASA test pilot was used to evaluate changes to the approach guidance resulting from the various combinations of position difference solutions and time constants. The pilot's task was to fly an ILS approach to the runway using the computer-drawn runway on the primary flight display (fig. 1) and associated symbology (described in ref. 2) for guidance. The pilot was to subjectively evaluate changes to the guidance resulting from modifications to the position difference solutions and the position estimate time constants. To aid the pilot with this evaluation, a second computer-drawn runway was drawn on the primary flight display to represent the real-world runway as it would appear through a superimposed display of a forward-looking television image. The real-world runway had no simulated noise or position errors and was to be used for comparison with the computer-drawn runway based on the navigation position estimate.

The evaluation runs were made with both single- and dual-component difference solutions, both 30- and 50-sec position estimate time constants, and both modified ($K_3 = 0$) and unmodified ($K_3 = 1$) velocity estimate equations. Simulated radio noise was also included during these runs.

One set of runs was made with an initial lateral position estimate error of 1000 ft. This position offset was readily seen in the difference between the real-world runway and the computer-drawn runway. The pilot did not report any difficulties or confusion in using the approach guidance while the position estimate algorithm was nulling the position error. However, both the overshoot, which resulted from the use of the unmodified velocity estimate equations, and the undershoot, which was obtained with the dual-component solution, modified velocity equations, and 50-sec gains, were very apparent, as could be seen by the differences in alignment between the simulated real-world runway and the computer-drawn runway. The pilot reported that the misalignment of the computer-drawn runway would degrade its usefulness when flying closer than approximately 1 mile to the runway. The use of the single-component difference solution, the modified velocity equations, and the 30-sec time constants resulted in good runway alignment and provided adequate guidance information for flight to the runway threshold.

An additional set of runs were made with no initial position estimate error. The pilot was instructed to turn the airplane back and forth approximately 20° to either side of the runway centerline to judge the dynamics of the display symbology caused by track angle and lateral displacements of the airplane. The pilot judged the motion of the symbology during these maneuvers to be smooth and acceptable for approach guidance for all runs.

Flight Tests

Test procedure.- Flight tests were conducted to validate the results obtained from the simulation tests. The TSRV 737 airplane was flown on a series of ILS approaches to runway 13 at the Federal Aviation Administration Technical Center (FAATC) airport located near Atlantic City, N.J. Ground-based precision radar tracking data were recorded to define the actual position of the airplane during each test run. During postflight data analysis, the vectorial difference between the radar-defined position and the onboard estimated position was computed and resolved into longitudinal (parallel to the runway centerline) and lateral (perpendicular to the runway centerline) components. The locations of the DME's used during these tests (fig. 10) resulted in the lateral difference component being influenced primarily by the ILS localizer signals and the longitudinal difference component being influenced by the DME signals.

Figure 10 shows the flight path used during these tests. The path was programmed into the area navigation system to provide tracking guidance for the pilot to intercept the ILS localizer at a point 10 to 15 n.mi. from the localizer antenna. Position estimates computed during the flight to the final approach path used inertial velocity and either dual- or single-DME inputs, depending on the signal and geometrical validity requirements programmed into the navigation system. The algorithms used during this process are described in reference 3.

Once the ILS localizer was intercepted, the pilot would slow the airplane to approximately 140 knots and maintain level flight at an altitude of 3500 ft. Radar and airborne data recording were begun prior to passing waypoint ILS10, which was located 10 n.mi. from the localizer antenna. After passing waypoint ILS10, the navigation position estimate was computed using the ILS and DME information. Once the glide slope was intercepted, the pilot used ILS localizer and glide slope deviation information for guidance since these were unaffected by the position estimate errors artificially induced for these flight tests. Each test run was complete once the airplane crossed the approach threshold of the runway.

During the test run, when the airplane was approximately 8 n.mi. from the localizer antenna, the flight test engineer inserted an incremental change in the position estimate which resulted in a 1000-ft right lateral shift (relative to the ILS localizer) and a 1000-ft rearward longitudinal shift. The convergence characteristics resulting from the correction of these induced errors were quantified with the same parameters used in the simulation tests.

A subjective evaluation was made by a NASA test pilot to determine if the guidance based on the navigation position estimate was adversely affected by the modified estimate algorithms and the faster filter time constants. The evaluation was based primarily on a comparison of the computer-drawn runway with the real-world runway television image superimposed on the primary flight display.

Functional check.- An initial test run was flown to conduct a functional check of the airborne software and to determine that adequate DME signal coverage was available for these flight tests. During this initial test run, ILS localizer and DME signals were used 93 percent of the time to compute the position estimate. During the remainder of the test run, inputs from the DME receiver were not valid and the position estimates were computed with localizer inputs only (ILX mode).

The automatic tuning feature of the navigation system has been programmed to select DME radio stations that meet both geometric criteria programmed in the NCU (ref. 6) and signal validity based on the quality and strength of the received signal programmed in the radio receiver. The data recorded on the airplane indicated that the Atlantic City (ACY) DME was used throughout most of the test run. However, the DME signal was intermittently invalid and caused the Cedar Lake (VCN) DME to be automatically tuned during the last 49 sec of the functional check.

Lateral convergence.- The lateral convergence characteristics of the position estimate for an offset of approximately 1000 ft for the various position estimate algorithm configurations flight tested (i.e., magnitude of K_3, position difference solution, and filter time constant) are summarized in table III. The length of time of each test and the percent of time that both ILS localizer and DME inputs were used to compute the position estimate are also shown in table III. A single offset was induced on five runs and two offsets were induced on an additional two runs (denoted a and b).

The lateral convergence characteristics obtained from the flight tests were similar to those obtained for the same algorithm configuration and filter time constants used during the simulation tests. The values of the offset obtained at the end of each run were generally greater during the flight test than during simulation. This was partly because the elapsed time of each flight test was shorter than the 169 sec used during the simulation test runs. (A tail wind component was encountered during the flight tests which resulted in higher ground speeds and subsequently shorter times to fly to the runway.) In addition, during the DME signal dropouts, the position estimate was computed in the ILX mode.

Figure 11 shows plots of lateral displacement as a function of time for four flight test runs. These plots are similar to those obtained during the simulation tests. Test run 1 was conducted with the original dual-component position estimate algorithm, a 50-sec filter time constant, and K_3 set equal to 1. This configuration resulted in the slowest convergence of the lateral displacement. Test run 2 was conducted with the single-component position estimate, a 50-sec filter time constant, and K_3 set equal to 1. The higher rate of convergence (compared to test run 1) shown on this plot was due to the use of the single-component position estimate

TABLE III.- LATERAL CONVERGENCE CHARACTERISTICS OF ILS-DME POSITION ESTIMATE

[TSRV flight test]

Test run	Velocity estimate constant K_3	Position difference solution	Filter time constant, sec	Initial recovery rate, fps	63-percent recovery time, sec	Offset at end of run,* ft	Elapsed time of test, sec	Time in ILD update mode, percent
1	1	Dual component	50	18.8	34.8	342**	44**	67
2	1	Single component	50	47.5	20.5	-50	122	97
3	1	Single component	30	58.8	14.3	10	109	59
4a	1	Single component	30	54.4	14.9	48	70	53
4b	1	Single component	30	55.6	14.3	116**	33**	82
5a	0	Single component	30	61.3	12.2	60**	46**	67
5b	0	Single component	30	56.3	14.4	105**	48**	31
6	0	Single component	30	58.5	14.3	10	93	73
7	0	Single component	30	54.1	15.4	10	98	75

*Negative offset indicates an overshoot.
**Insufficient time remaining in test run for lateral convergence to be completed.

algorithm. However, the lateral error was reduced only to approximately 20 ft and then increased and remained at 40 ft until the completion of the test. Test runs 3 and 6 were conducted with the single-component position estimate and a 30-sec filter time constant. For test run 3, K_3 was set equal to 1 and for test run 6 it was set equal to 0. The lateral convergence was faster on these runs than on run 2 due to the use of the quicker time filter constant. The lateral error was nulled smoothly (to 10 ft at the end of the test) on run 3. The lateral error on run 6 was also smooth but converged to a 35-ft standoff error. This error was maintained for about 30 sec before converging to 10 ft. This standoff error may be attributed to loss of the DME signal, which resulted in the use of the ILX mode.

The pilot reported no adverse effects to the approach guidance from modifications to the position estimate algorithm. The dynamics of the computer-drawn runway displayed on the electronic attitude director indicator were smooth with both 30- and 50-sec filter time constants.

Longitudinal convergence.- The longitudinal convergence rates were almost identical to those obtained on the lateral axis when the DME signals were valid. When the DME signals were invalid, the position estimate was computed with ILS localizer signals and the longitudinal recovery rate dropped to zero.

Figure 12 shows plots of the longitudinal displacement as a function of time for two of the flight test runs. Both runs were configured using the single-component position estimate with a 30-sec filter time constant. The plateaus where the longitudinal displacement did not change indicate the times during which the DME signals were invalid. In run 3, K_3 was set equal to 1 and in run 5a it was set equal to 0. It was anticipated that some overshoot would occur in run 3 ($K_3 = 1$) because of the overshoot obtained in the simulator (table I). However, none of the flight test runs resulted in the longitudinal error converging to zero, which indicated that a bias error could be present in the DME system.

In an effort to determine the combined accuracy of the airborne and ground DME systems, a comparison was made between the DME value measured on the airplane and a calculated distance determined from the location of the airplane (defined by the precision radar tracking data) and the known location of the DME ground facility. Slant range error due to the difference in altitude between the airplane and the DME station was taken into account. This analysis showed that the indicated DME values measured on the airplane were greater than the theoretical values obtained from both DME ground stations used during the test runs. The mean error for all test runs was 739 ft and the standard deviation was 247 ft.

The DME ground stations used during these tests were standard radio navigation facilities normally used in the national airspace structure. Combined ground and airborne accuracy is specified as 0.5 n.mi. or 3 percent of the indicated distance, whichever is greater (ref. 7).

Although the DME system errors resulting during these tests are well within the specified accuracy tolerances for en route DME systems, the use of precision DME facilities may be required to compute guidance for precision approaches or for superimposition on real-world images (i.e., head-up or head-down displays with electronic real-world imagery). The NASA test pilot reported that the longitudinal error was only observable on the computer-drawn runway guidance when close to the runway threshold (within approximately 1 mile).

CONCLUDING REMARKS

The results from simulation tests showed that improvements to the convergence characteristics and accuracy of the TSRV area navigation system position estimate could be obtained through modifications to the position difference computations, the position estimate filter time constant, and the velocity estimate equations. Flight test results generally agreed with the simulator results except for the accuracy improvements obtained through modifications to the velocity estimate. Accuracy improvements with this modification are not evident in the flight data supported by radar tracking information. Lateral convergence (influenced by ILS localizer radio signals) in nulling an artifically induced position estimate error was substantially faster with the single-component position difference solution than with the dual-component solution. Convergence in the longitudinal axis (influenced by DME radio signals) was approximately the same for both solutions. Use of the 30-sec time constant filter gains resulted in approximately 66 percent faster convergence than was obtained with the 50-sec gains. During simulation tests an overshoot error in the

position estimate was eliminated by setting an accumulation term in the velocity estimate equations equal to zero.

The guidance drawn on the electronic flight displays was smooth for all position estimate algorithm configurations and filter time constants tested. It was noted that some longitudinal error could be detected between the computer-drawn runway and the superimposed real-world runway displayed on the electronic attitude director indicator when the airplane was close to the approach threshold of the runway. This longitudinal error was caused by a bias error in the DME indication used in the position difference equations. Although the bias error was within system tolerances for en route navigation DME, the use of precision DME may be required for approach to landing.

Langley Research Center
National Aeronautics and Space Administration
Hampton, VA 23665
January 12, 1984

APPENDIX A

POSITION ESTIMATE FILTER

The first step in the position estimate process is to develop a velocity estimate update from the north and east components of the position difference ($\Delta P_{N,t}, \Delta P_{E,t}$) obtained from the vector between the last previously estimated position and the position defined by the radio navigation information. Thus

$$\Delta V_{N,t} = K_3 \, \Delta V_{N,t-1} + K_2 \, \Delta P_{N,t} \quad \text{knots}$$

$$\Delta V_{E,t} = K_3 \, \Delta V_{E,t-1} + K_2 \, \Delta P_{E,t} \quad \text{knots}$$

where

$K_2 = 900 \, \Delta t / T^2 \quad \text{hr}^{-1}$

$K_3 = 1.0$

$\Delta t = 1/20$ sec

T = Time constant for position estimate filter

A velocity estimate is then made by summing the velocity update with ground speed obtained from the inertial navigation system:

$$V_{N,t} = \Delta V_{N,t} + \hat{V}_{N,t} \quad \text{knots}$$

$$V_{E,t} = \Delta V_{E,t} + \hat{V}_{E,t} \quad \text{knots}$$

A position update in terms of latitude and longitude is obtained from the system velocity and the position difference components as follows:

$$\Delta\phi_t = \left[\frac{(1/3600) V_{N,t} \, \Delta t + K_1 \, \Delta P_{N,t}}{r_{M,t}} \right] \frac{180}{\pi} \quad \text{deg}$$

$$\Delta\lambda_t = \left[\frac{(1/3600) V_{E,t} \, \Delta t + K_1 \, \Delta P_{E,t}}{r_{N,t}} \right] \frac{180}{\pi} \quad \text{deg}$$

where $K_1 = 2\ \Delta t/T$. This latitude and longitude position update is based on an oblate spheroid Earth model (ref. 3) using the following radii of curvature in the meridional (north-south) and normal (east-west) directions:

$$r_{M,t} = \left[h_{a,t} + r_E\left(1 - 2F + 3F \sin^2\phi_{e,t-1}\right)\right] \frac{1}{6076.1} \quad \text{n.mi.}$$

$$r_{N,t} = \left[h_{a,t} + r_E\left(1 + F \sin^2\phi_{e,t-1}\right) \cos \phi_{e,t-1}\right] \frac{1}{6076.1} \quad \text{n.mi.}$$

where

$$F = 0.003367$$

$$r_E = 20\ 925\ 873.79 \quad \text{ft}$$

The position estimate is found by summing the previous position estimate with the position update terms:

$$\phi_{e,t} = \phi_{e,t-1} + \Delta\phi_t \quad \text{deg}$$

$$\lambda_{e,t} = \lambda_{e,t-1} + \Delta\lambda_t \quad \text{deg}$$

APPENDIX B

ILS LOCALIZER-ONLY POSITION DIFFERENCE COMPONENT

General Solution

A position difference component may be computed from ILS localizer angular-deviation information. Figure B1 shows the geometry of the ILS localizer antenna, the runway with an extended centerline, the last estimated position of the airplane $(\phi_e,\lambda_e)_{t-1}$, and its estimated position on a measured localizer radial. An orthogonal coordinate system with its origin at the localizer antenna (ϕ_o,λ_o) is oriented toward true north.

A vector $\overrightarrow{DP}_t$ was found by subtracting the vector $\vec{Z}_{e,t-1}$ (defined from the localizer antenna to the location of the last position estimate) from the vector $\vec{Z}_{r,t}$ (defined from the localizer antenna along the measured ILS localizer radial and having the same length as vector $\vec{Z}_{e,t-1}$). A vector component $\overrightarrow{DP}_{p,t}$ perpendicular to the runway centerline was computed from the position difference vector $\overrightarrow{DP}_t$. Then $\overrightarrow{DP}_{p,t}$ was broken into north and east components for use in the position estimate computations.

Calculation of $\overrightarrow{DP}_t$

To determine $\overrightarrow{DP}_t$ it was necessary to calculate the north and east components of position estimate vector $\vec{Z}_{e,t-1}$ from the latitudes and longitudes of the last position estimate and the ILS localizer antenna location:

$$Z_{e,N,t-1} = 60(\phi_{e,t-1} - \phi_o) \quad \text{n.mi.}$$

$$Z_{e,E,t-1} = 60(\lambda_{e,t-1} - \lambda_o) \cos \frac{\phi_{e,t-1} + \phi_o}{2} \quad \text{n.mi.}$$

Thus

$$\vec{Z}_{e,t-1} = (Z_{e,E,t-1})\hat{i} + (Z_{e,N,t-1})\hat{j} \quad \text{n.mi.}$$

A vector $\vec{Z}_{r,t}$ of the estimated position of the airplane along a measured localizer radial was determined in the following manner. Since no radio-based range information could be obtained along a radial from the ILS localizer antenna, the

magnitude of $\vec{Z}_{r,t}$ was chosen to be equal to the magnitude of $\vec{Z}_{e,t-1}$. The length of $\vec{Z}_{r,t}$ and $\vec{Z}_{e,t-1}$ was

$$Z_{r,t} = Z_{e,t-1} = \left[\left(Z_{e,N,t-1}\right)^2 + \left(Z_{e,E,t-1}\right)^2\right]^{1/2} \quad \text{n.mi.}$$

The north and east components of $\vec{Z}_{r,t}$ were found from the angle $\psi_r - \eta_t$ between the vector $\vec{Z}_{r,t}$ and the north axis:

$$Z_{r,N,t} = Z_{r,t} \cos(\psi_r - \eta_t) \quad \text{n.mi.}$$

$$Z_{r,E,t} = Z_{r,t} \sin(\psi_r - \eta_t) \quad \text{n.mi.}$$

Thus

$$\vec{Z}_{r,t} = (Z_{r,E,t})\hat{i} + (Z_{r,N,t})\hat{j} \quad \text{n.mi.}$$

The position difference vector $\overrightarrow{DP}_t$ was found as follows:

$$\overrightarrow{DP}_t = \vec{Z}_{r,t} - \vec{Z}_{e,t-1}$$

Calculation of Position Difference $\Delta P_{N,t}, \Delta P_{E,t}$

The magnitude of the component $\overrightarrow{DP}_{p,t}$ of $\overrightarrow{DP}_t$ perpendicular to the runway centerline was obtained from the dot product of $\overrightarrow{DP}_t$ and a unit vector $\hat{u}$ perpendicular to the runway centerline. The unit vector $\hat{u}$ was defined as

$$\hat{u} = -\cos(\psi_r)\hat{i} + \sin(\psi_r)\hat{j}$$

The magnitude of $\overrightarrow{DP}_{p,t}$ was thus

$$DP_{p,t} = \overrightarrow{DP}_t \cdot \hat{u} \quad \text{n.mi.}$$

$$= -(Z_{r,E,t} - Z_{e,E,t-1}) \cos \psi_r + (Z_{r,N,t} - Z_{e,N,t-1}) \sin \psi_r \quad \text{n.mi.}$$

The north and east components of $\overrightarrow{DP}_{p,t}$ were

$$\Delta P_{N,t} = DP_{p,t} \sin \psi_r \quad \text{n.mi.}$$

$$\Delta P_{E,t} = -DP_{p,t} \cos \psi_r \quad \text{n.mi.}$$

These position difference components were used directly in the navigation position estimate algorithms.

APPENDIX B

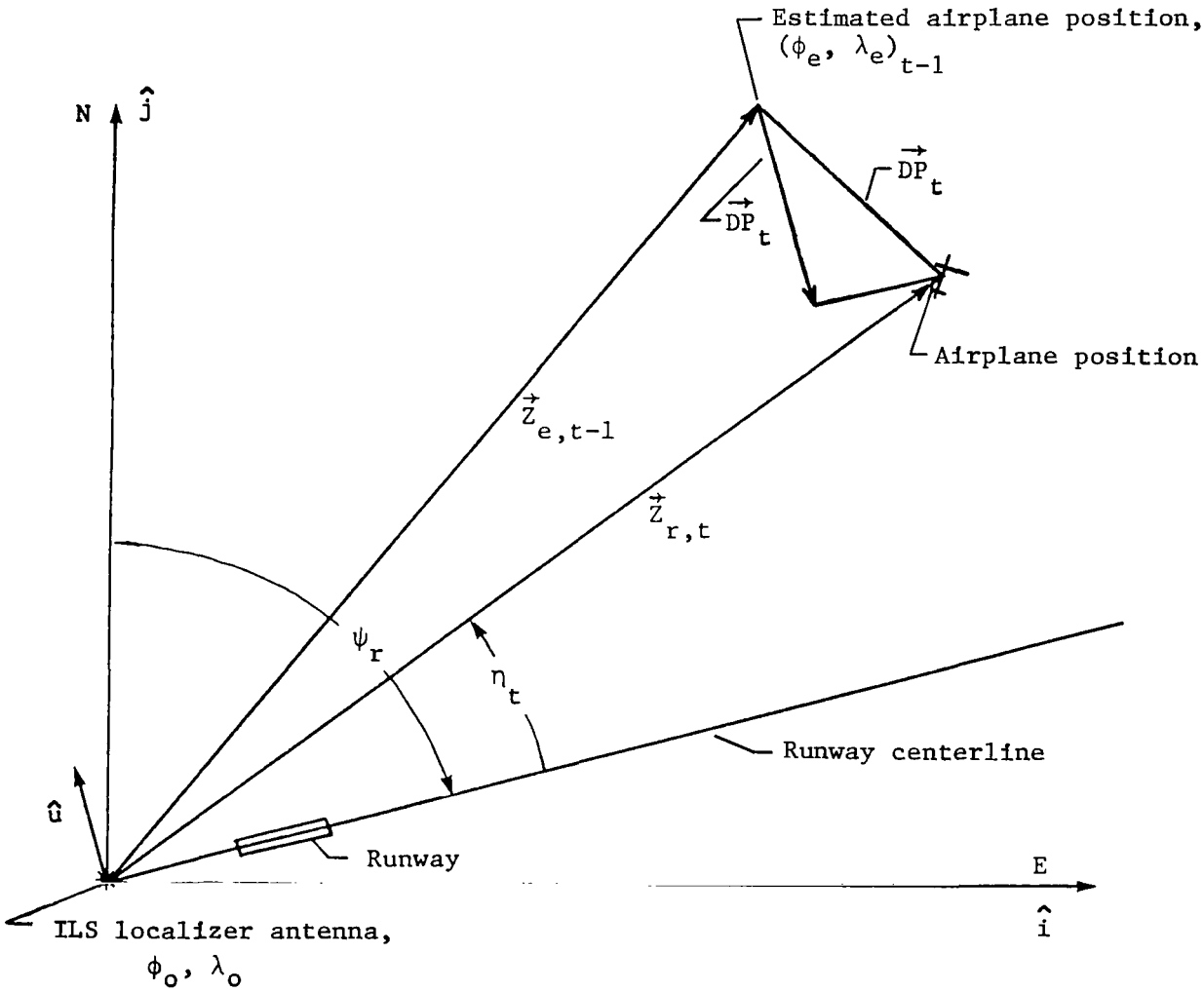

Figure B1.- Geometry pertaining to ILX position estimate mode.

REFERENCES

1. Walsh, Thomas M.; and Weener, Earl F.: Automatic Flight Performance of a Transport Airplane on Complex Microwave Landing System Paths. Guidance and Control Design Considerations for Low-Altitude and Terminal-Area Flight, AGARD-CP-240, Apr. 1978, pp. 19-1 - 19-12.

2. Morello, Samuel A.; Knox, Charles E.; and Steinmetz, George G.: Flight-Test Evaluation of Two Electronic Display Formats for Approach to Landing Under Instrument Conditions. NASA TP-1085, 1977.

3. Cosley, D.; and Martin, A. J.: SST Technology Follow-On Program - Phase II. ADEDS Functional/Software Requirements. Rep. No. FAA-SS-73-19, Dec. 1973. (Available from DTIC as AD B000 287.)

4. Knox, Charles E.: Algorithms and Logic for Incorporating ILS Localizer Information Into the NASA TCV B-737 Airplane Area Navigation System. NASA TM-80167, 1979.

5. Luciani, V. J.: NAFEC Range Instrumentation Systems. Rep. No. FAA-NA-79-32, Feb. 1980.

6. Giroir, L.; Martin, A.; Paulson, V.; and Peal, R.: SST Technology Follow-On Program - Phase II. ADEDS Interface Description. Rep. No. FAA-SS-73-20, Mar. 1974. (Available from DTIC as AD 920 805.)

7. Airman's Information Manual - Basic Flight Information and ATC Procedures. FAA, Nov. 24, 1983.

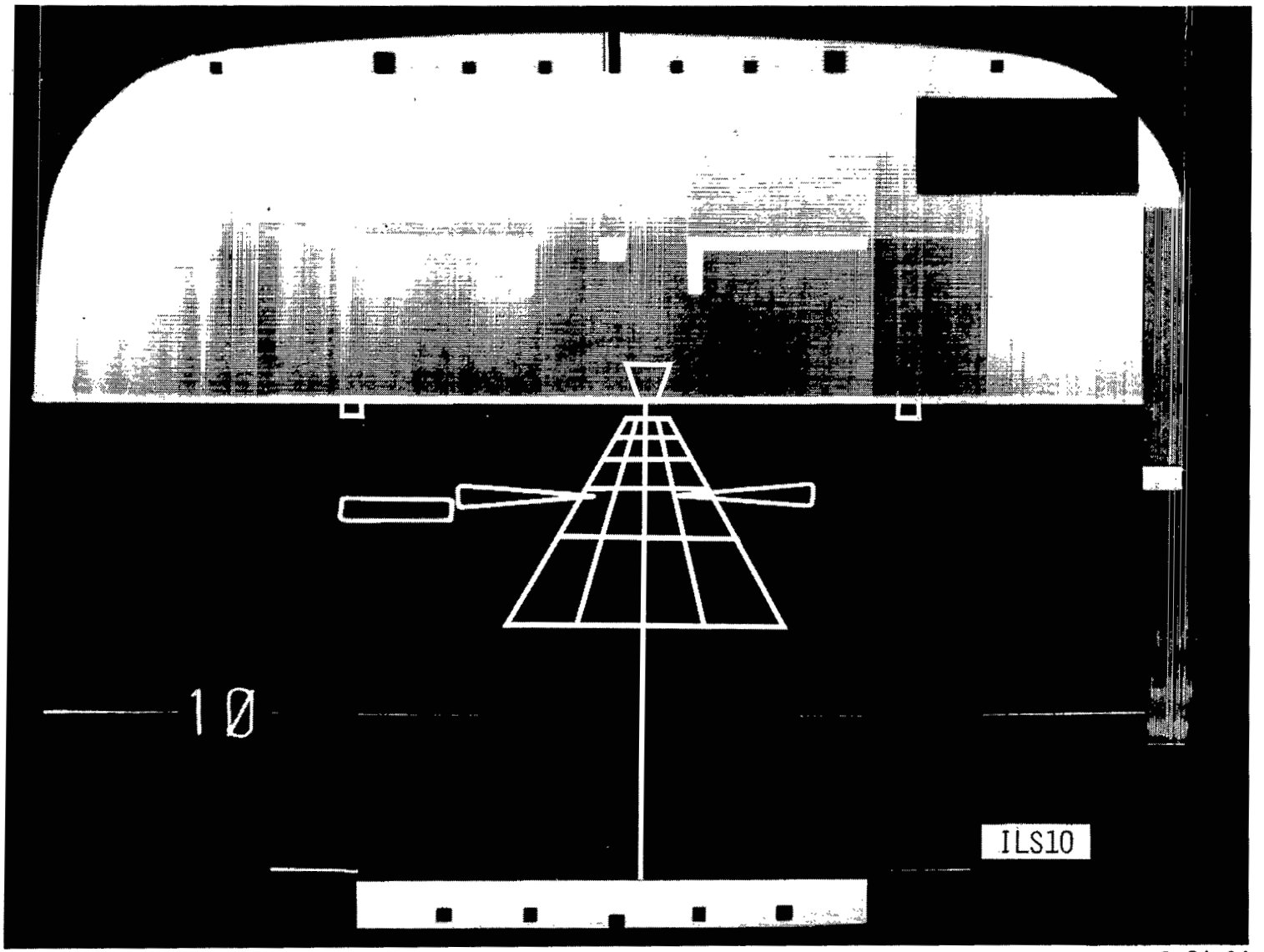

L-84-04

Figure 1.- Computer-drawn runway on electronic primary flight display.

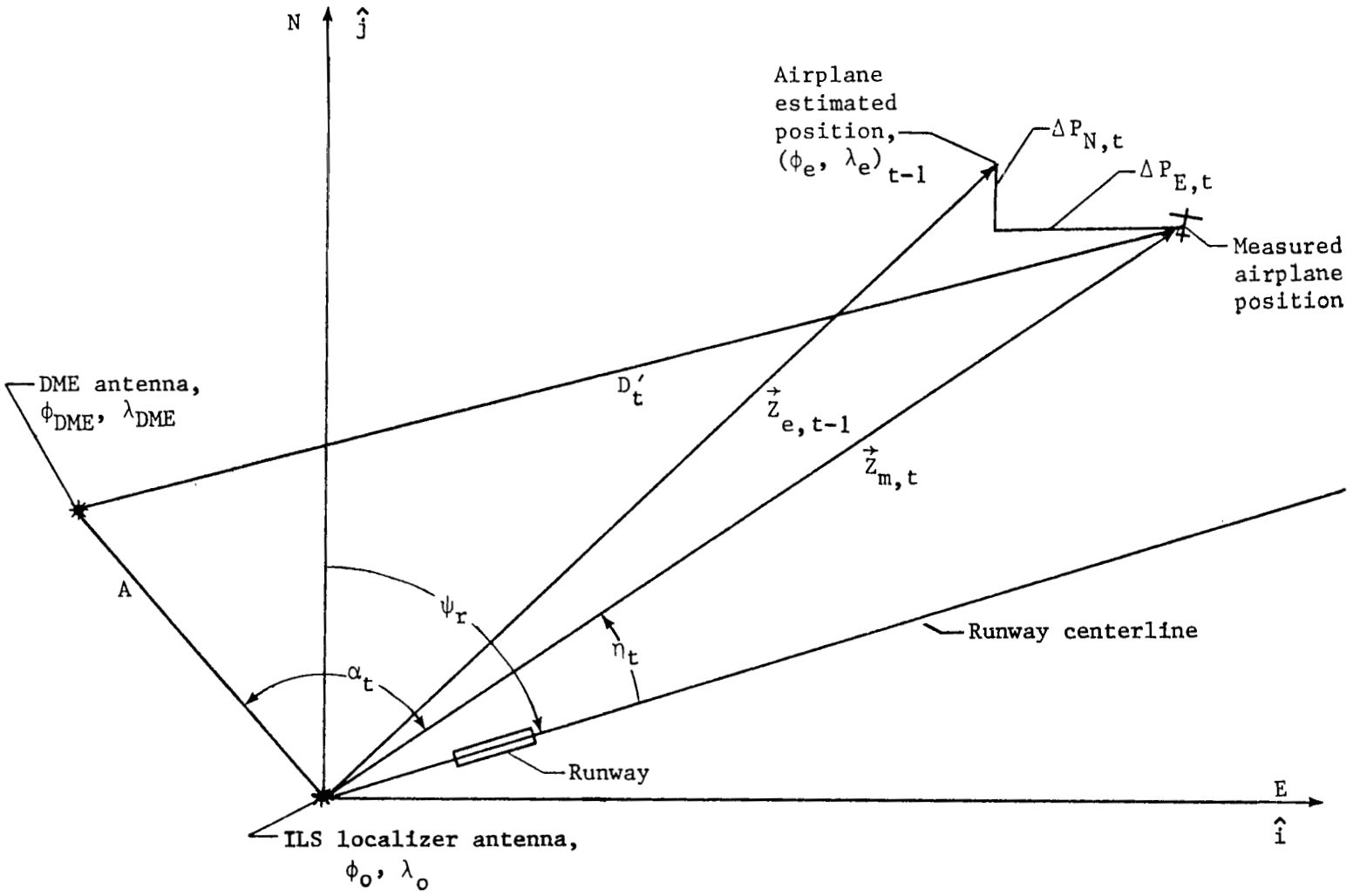

Figure 2.- Geometry pertaining to ILD single-component position estimate: ILS localizer antenna, DME, estimated and measured positions of airplane, and runway with extended centerline.

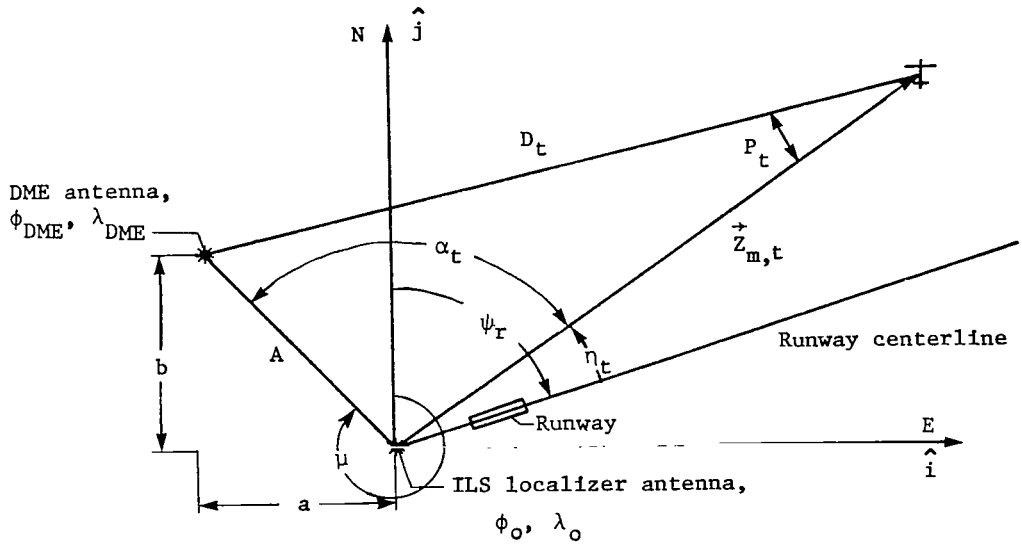

Figure 3.- Components of vector $\vec{Z}_{m,t}$ triangle used in ILD single-component position estimate.

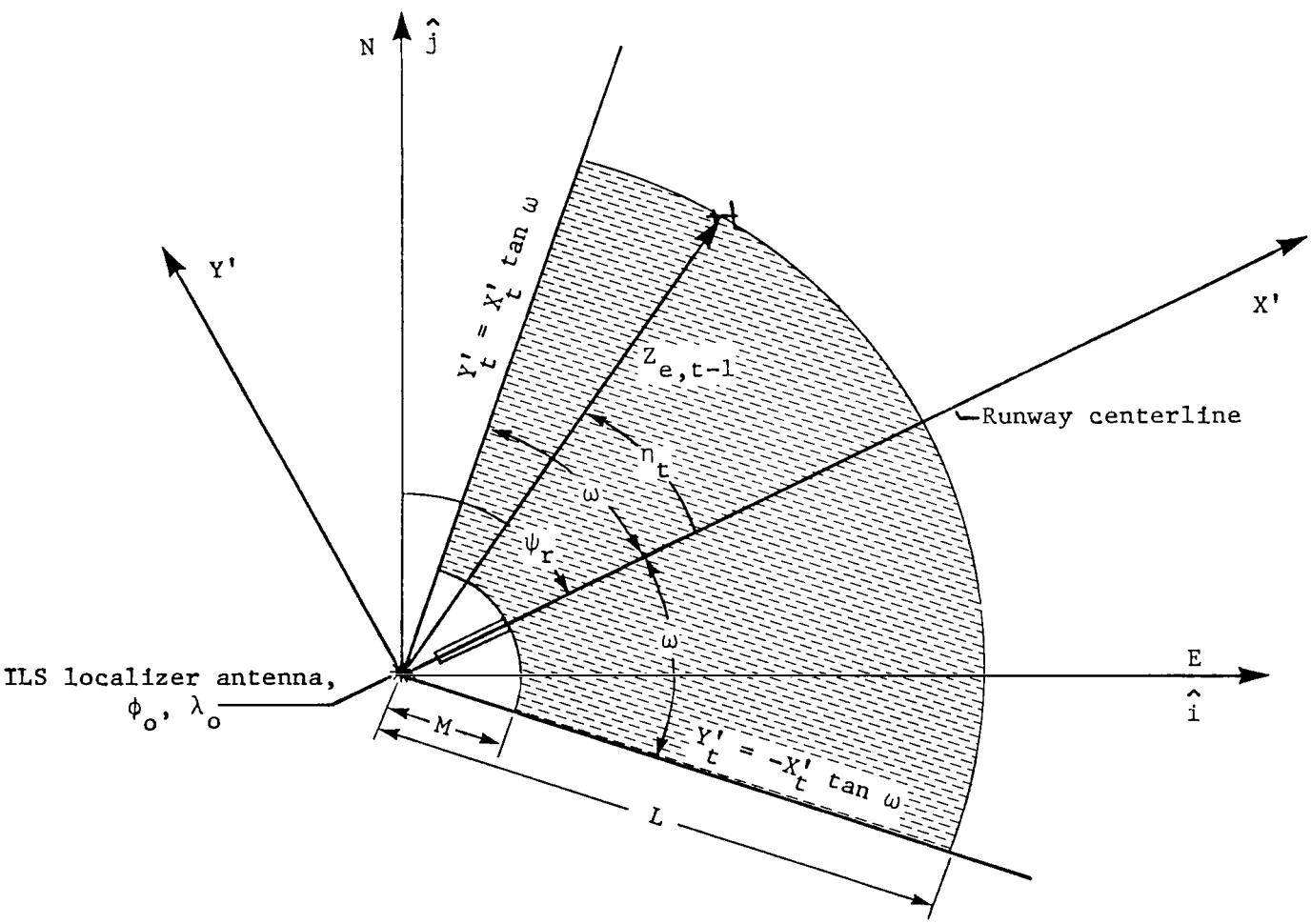

Figure 4.- Lateral and radial limits of ILS localizer geometry.

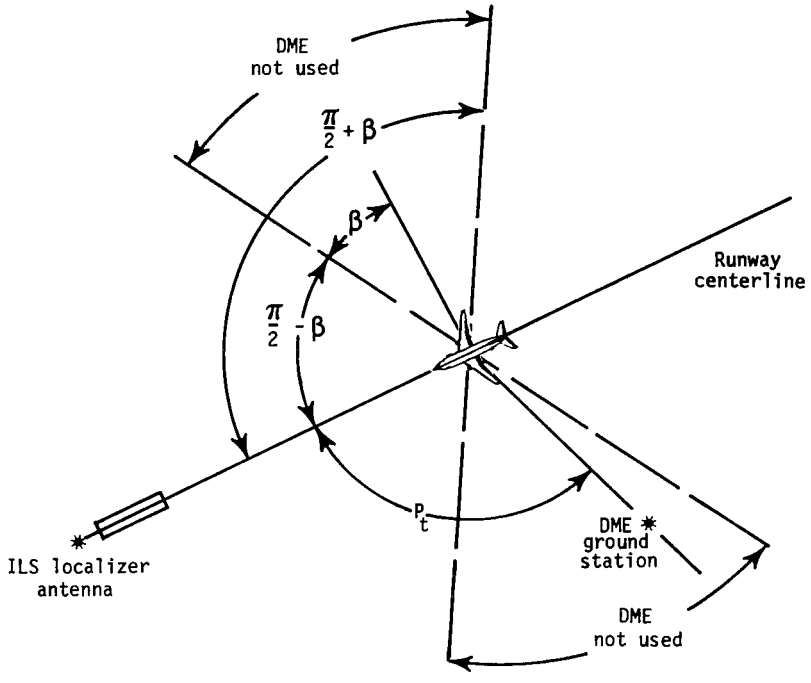

Figure 5.- DME ground station geometry check for ILD position estimate.

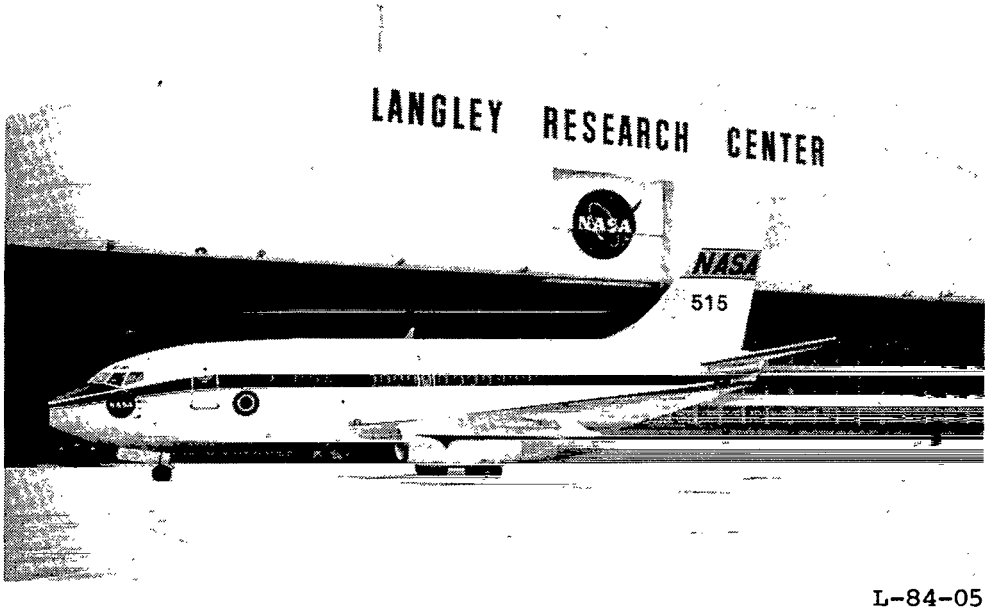

L-84-05

Figure 6.- Transport Systems Research Vehicle (TSRV).

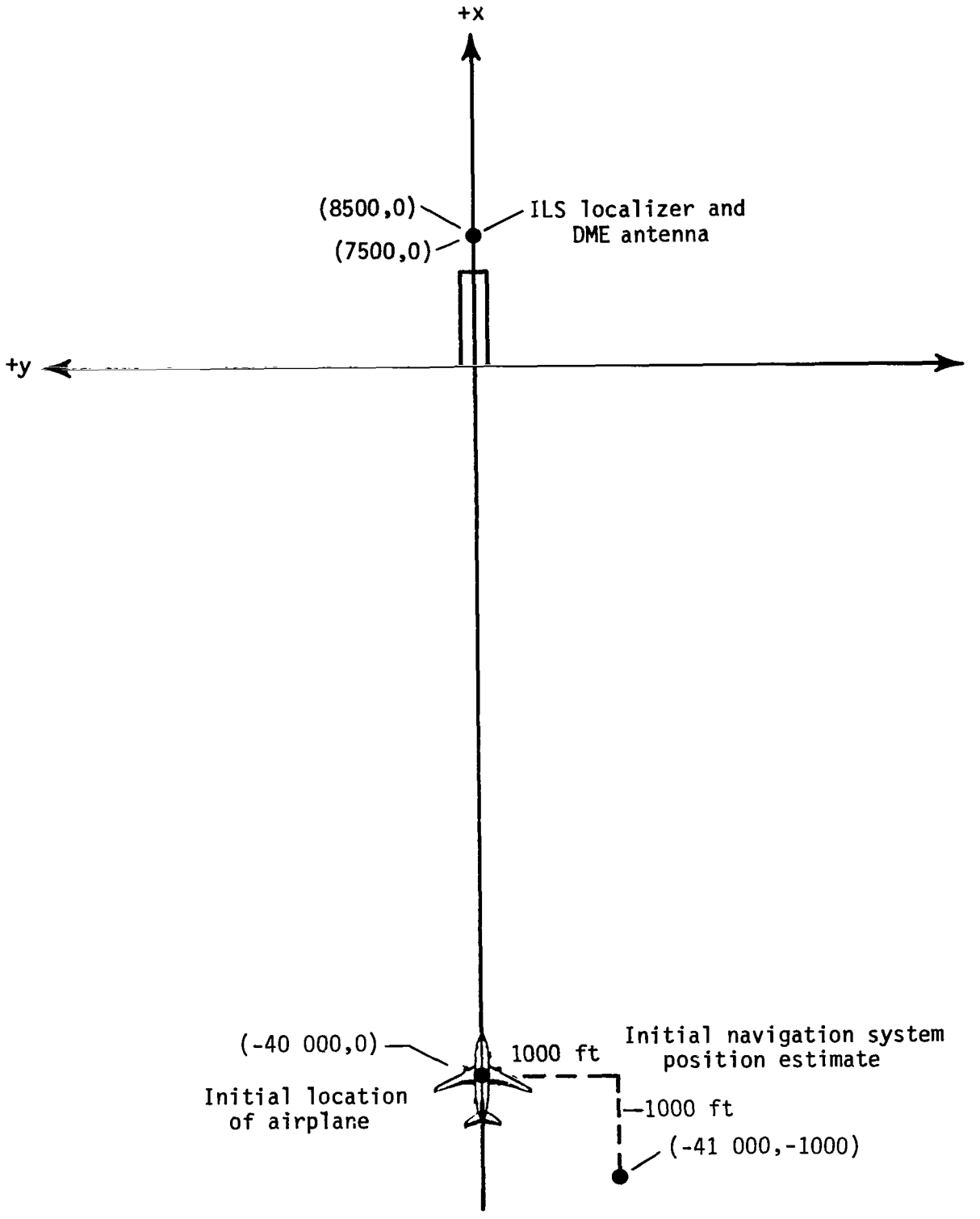

Figure 7.- Plan view of reference coordinate system and initial simulation test setup.

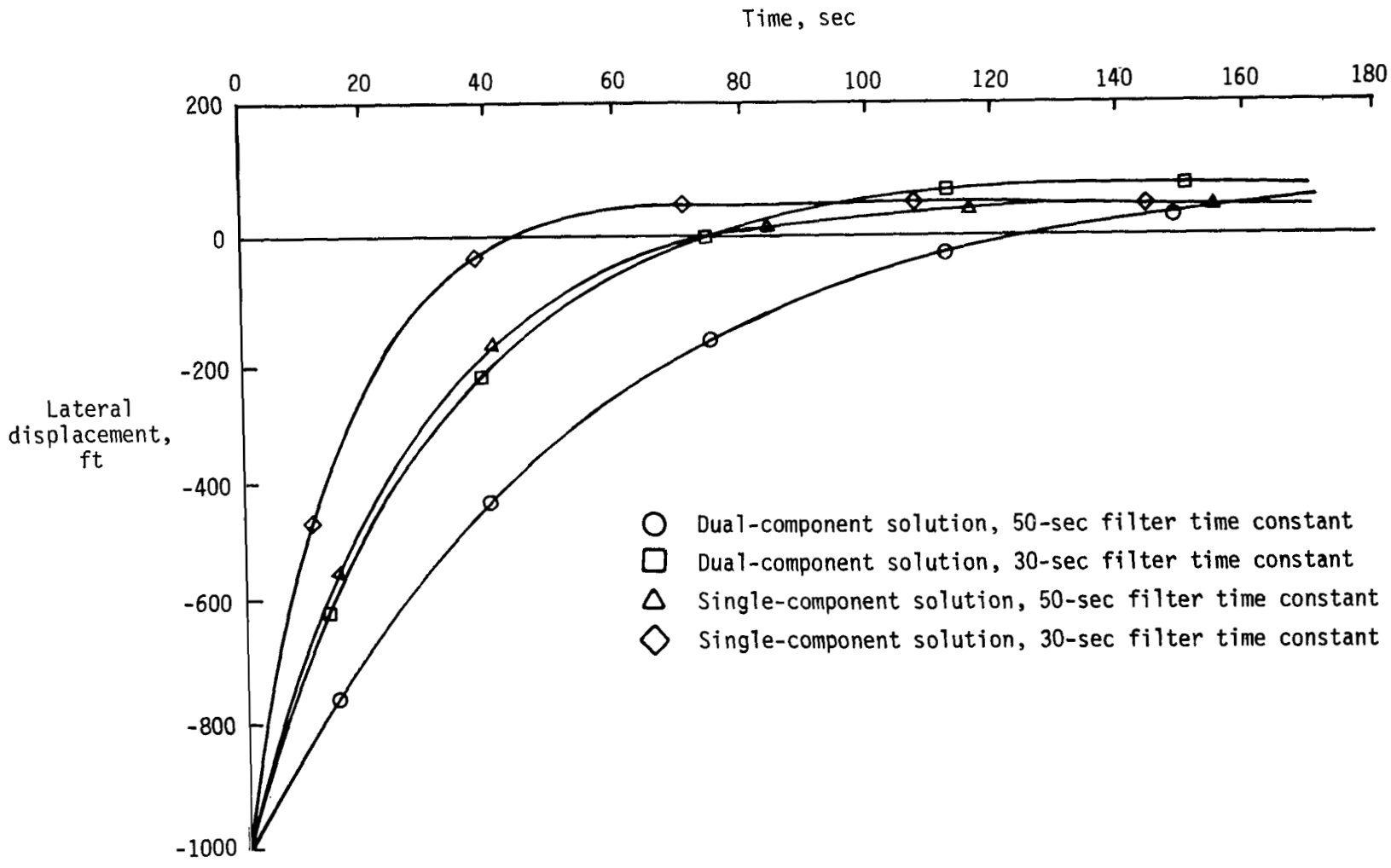

Figure 8.- Lateral component of position estimate error. TSRV simulation; $K_3 = 1$.

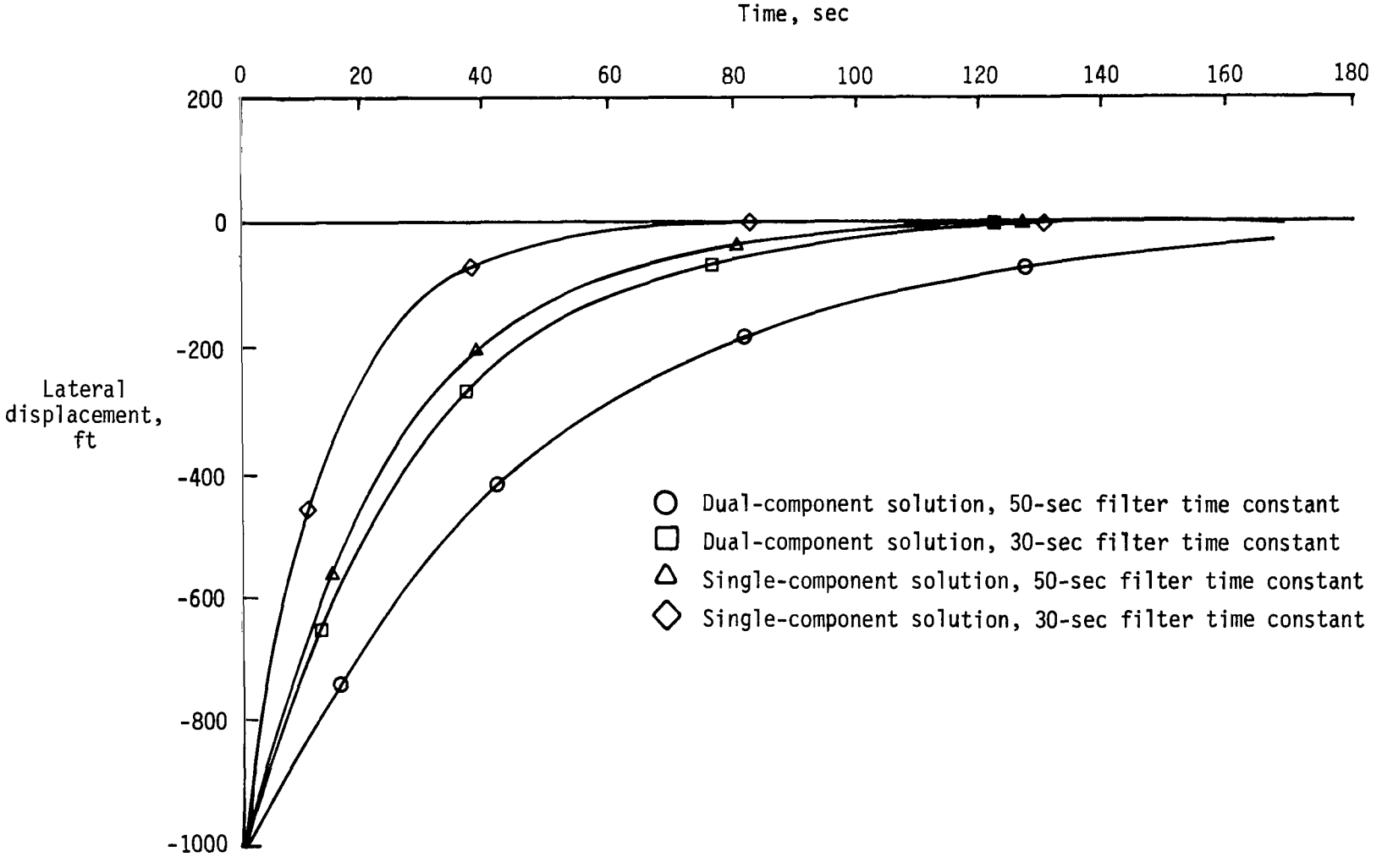

Figure 9.- Lateral component of position estimate error. TSRV simulation; $K_3 = 0$.

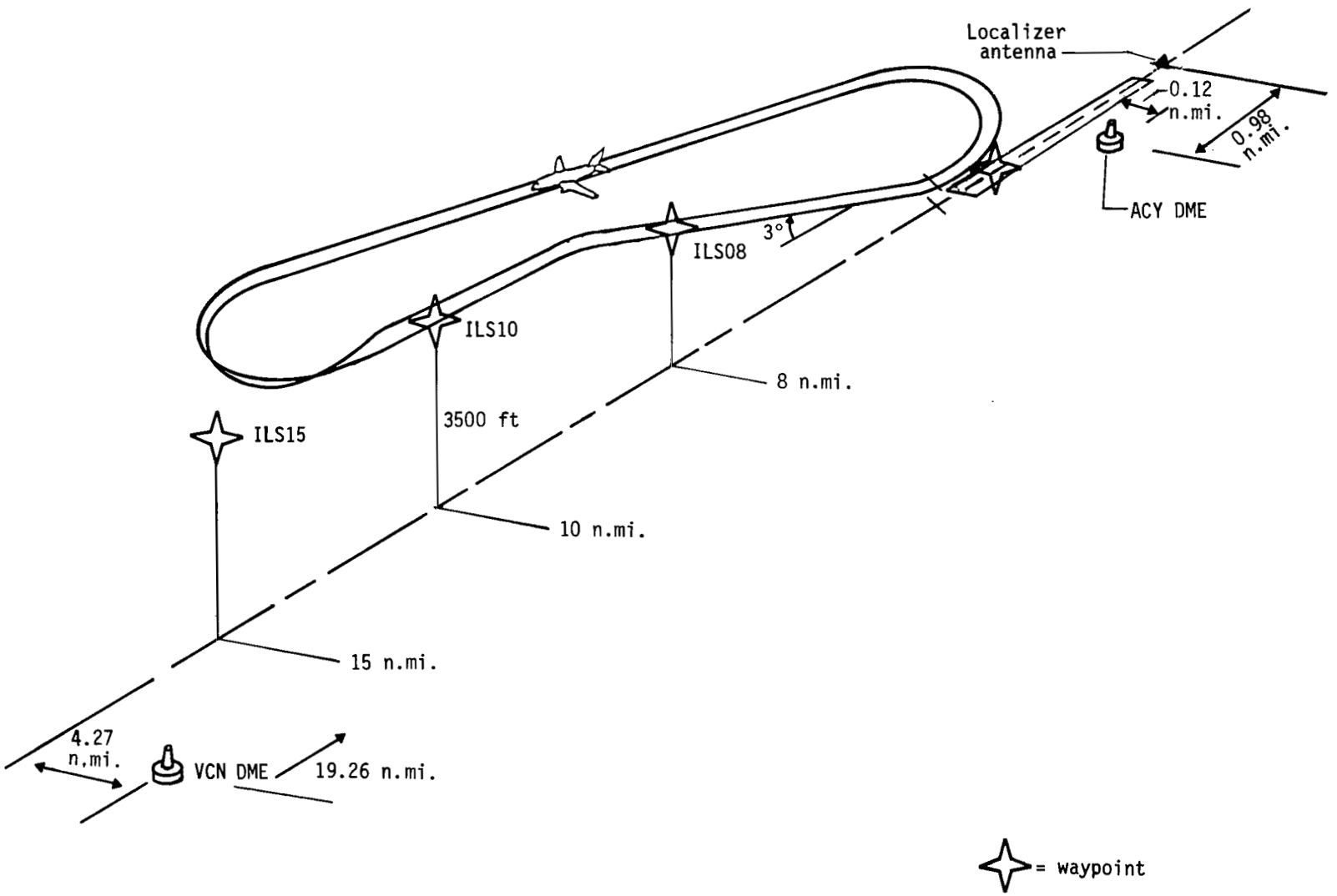

Figure 10.- Flight path at Atlantic City.

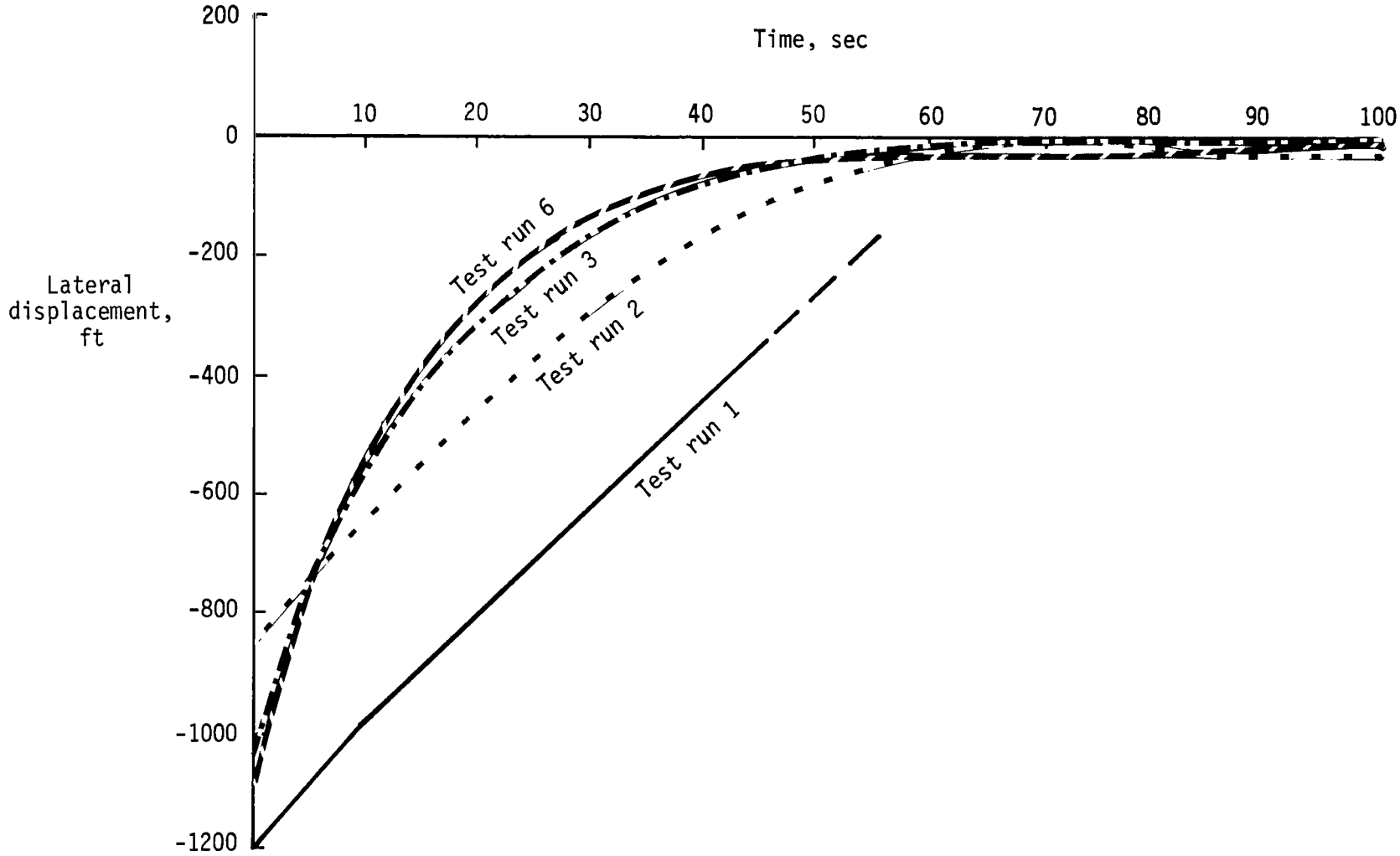

Figure 11.- Lateral component of ILS-DME position estimate. TSRV flight test.

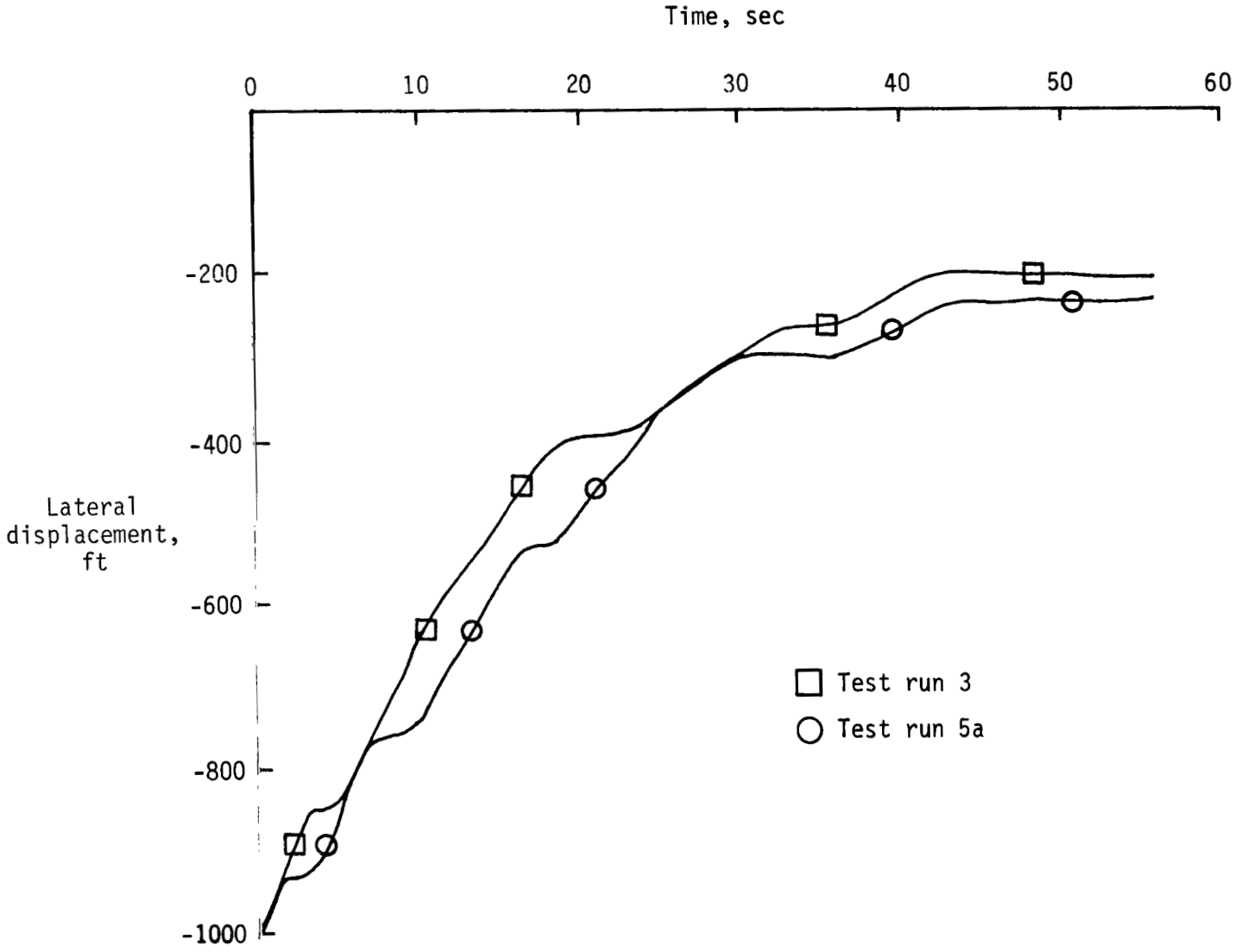

Figure 12.- Longitudinal component of ILS-DME position estimate. TSRV flight test.

1. Report No.	2. Government Accession No.	3. Recipient's Catalog No.
NASA TP-2281		

4. Title and Subtitle
A COMPARISON OF TWO POSITION ESTIMATE ALGORITHMS THAT USE ILS LOCALIZER AND DME INFORMATION - SIMULATION AND FLIGHT TEST RESULTS

5. Report Date
February 1984

6. Performing Organization Code
534-04-13-52

7. Author(s)
Charles E. Knox, Dan D. Vicroy, and Charles Scanlon

8. Performing Organization Report No.
L-15711

10. Work Unit No.

9. Performing Organization Name and Address
NASA Langley Research Center
Hampton, VA 23665

11. Contract or Grant No.

13. Type of Report and Period Covered
Technical Paper

12. Sponsoring Agency Name and Address
National Aeronautics and Space Administration
Washington, DC 20546

14. Sponsoring Agency Code

15. Supplementary Notes
Charles E. Knox and Dan D. Vicroy: Langley Research Center, Hampton, Virginia.
Charles Scanlon: Arkansas State University, State University, Arkansas.

16. Abstract

Simulation and flight tests were conducted to compare the accuracy of two algorithms designed to compute a position estimate with an airborne navigation computer. Both algorithms used ILS localizer and DME radio signals to compute a position difference vector to be used as an input to the navigation computer position estimate filter. The results of these tests show that the position estimate accuracy and response to artificially induced errors are improved when the position estimate is computed by an algorithm that geometrically combines DME and ILS localizer information to form a single component of error rather than by an algorithm that produces two independent components of error, one from a DME input and the other from the ILS localizer input.

17. Key Words (Suggested by Author(s))	18. Distribution Statement
Airplane guidance Airplane navigation Instrument Landing System Approach guidance Area navigation	Unclassified - Unlimited Subject Category 04

19. Security Classif. (of this report)	20. Security Classif. (of this page)	21. No. of Pages	22. Price
Unclassified	Unclassified	37	A03

For sale by the National Technical Information Service, Springfield, Virginia 22161

NASA-Langley, 1984

National Aeronautics and
Space Administration

Washington, D.C.
20546

Official Business
Penalty for Private Use, $300

THIRD-CLASS BULK RATE

Postage and Fees Paid
National Aeronautics and
Space Administration
NASA-451

1 1U,A, 840203 S00903DS
DEPT OF THE AIR FORCE
AF WEAPONS LABORATORY
ATTN: TECHNICAL LIBRARY (SUL)
KIRTLAND AFB NM 87117

NASA

POSTMASTER: If Undeliverable (Section 158 Postal Manual) Do Not Return